Electronic Supplementary Material (ESI) for Nanoscale.

Supporting Information

Atomic-Layered V_2C MXene Containing Bismuth Elements: 2D/0D and 2D/2D Nanoarchitectonics for Hydrogen Evolution and Nitrogen Reduction Reaction

Sana Akir*, Jalal Azadmanjiri, Nikolas Antonatos, Lukáš Děkanovský, Pradip Kumar Roy, Vlastimil Mazánek, Roussin Lontio Fomekong, Jakub Regner, Zdeněk Sofer*

Department of Inorganic Chemistry, University of Chemistry and Technology Prague, Technická 5, 166 28 Prague 6, Czech Republic

Email: akirs@vscht.cz , zdenek.sofer@vscht.cz

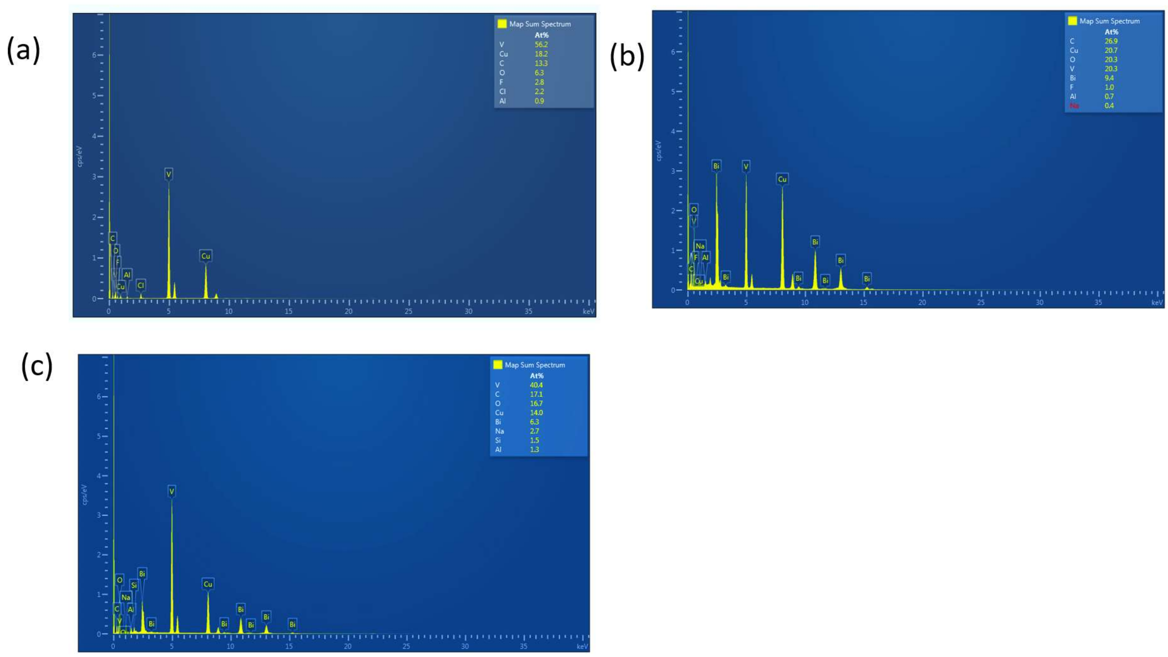

Fig. S1 EDS of (a) V_2C, (b) V_2C/BVO and (c) V_2C/Bi.

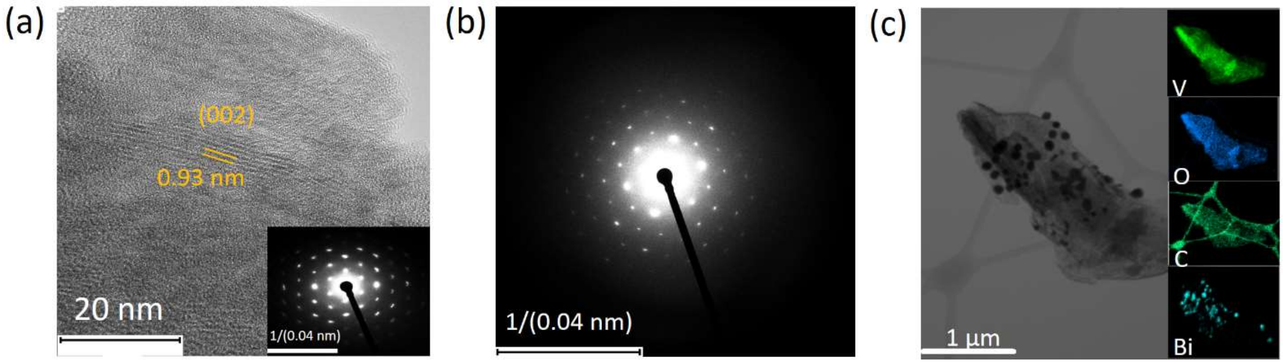

Fig. S2 (a) HRTEM of V_2C (inset SAED of V_2C), (b) SAED of V_2C/BVO and (c) the main elemental components mappings of V, O, C, and Bi of V_2C/Bi.

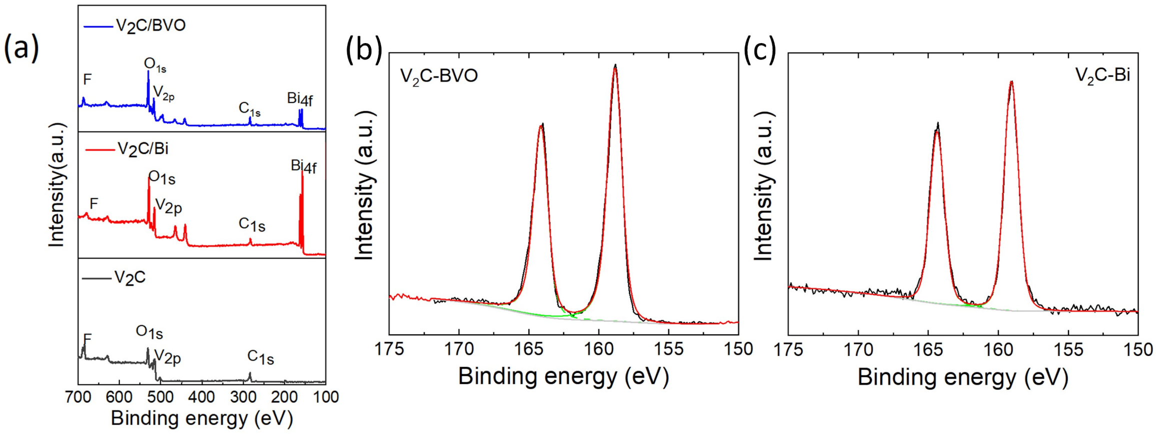

Fig. S3 (a) XPS survey spectra of catalysts, high-resolution XPS spectra of Bi 4f in (b) V_2C/BVO, and (c) V_2C/Bi.

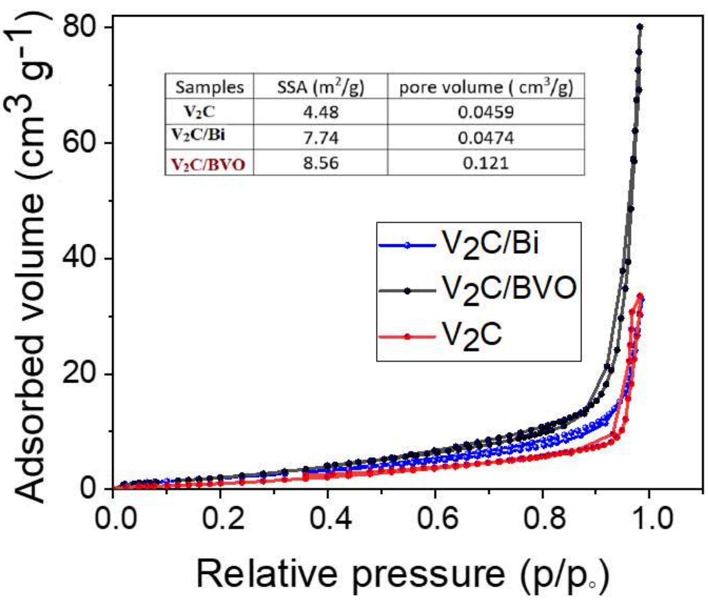

Fig. S4 Nitrogen adsorption-desorption isotherms of V_2C, V_2C/BVO, and V_2C/Bi, inset pore volume of catalysts.

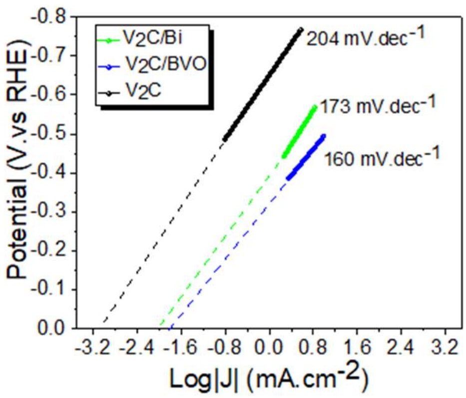

Fig. S5 Extended linear Tafel plots to determine the exchange current density of catalysts.

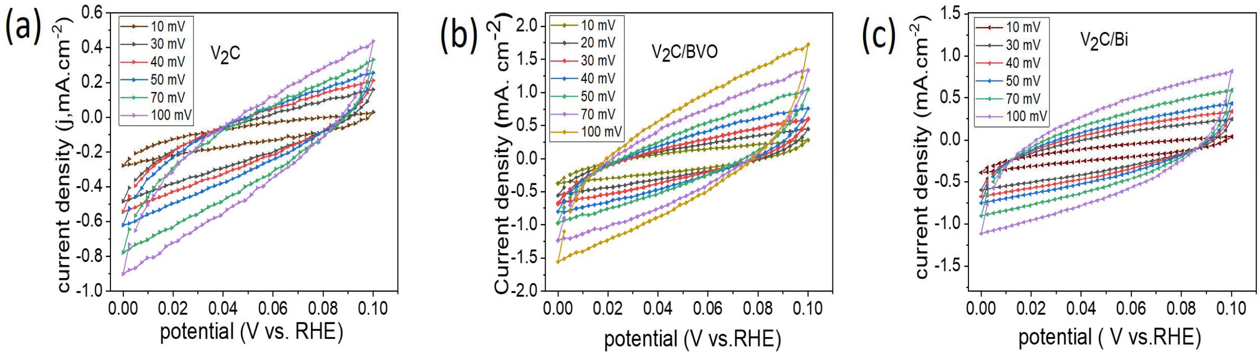

Fig. S6 Cyclic voltammograms obtained from the non-Faradic Region of (a) V_2C, (b) V_2C/BVO and (c) V_2C/Bi at different scan rates in H_2SO_4 (0.5M).

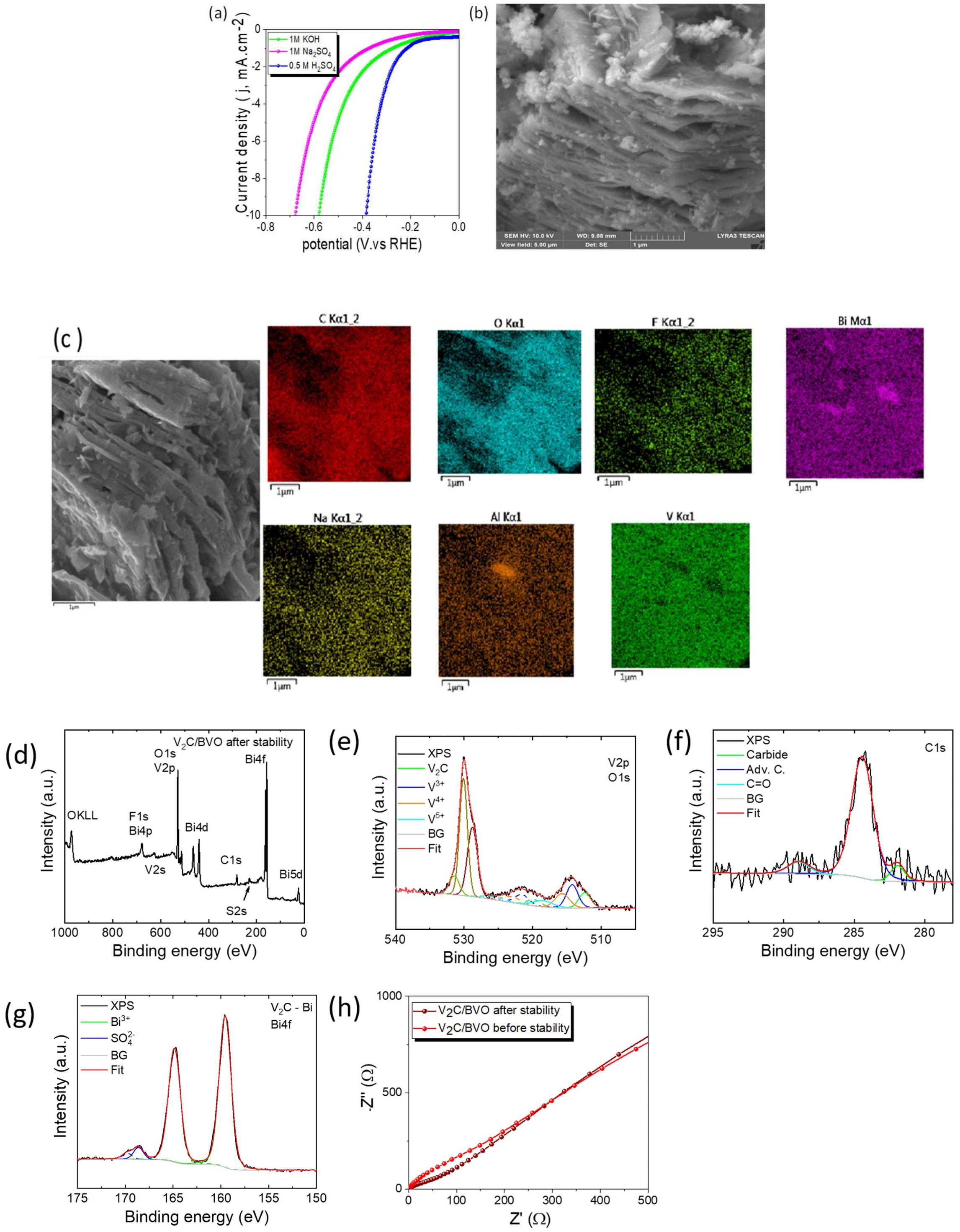

Fig. S7 (a) Linear sweep voltammetry (LSV) measurements of V_2C/BVO in 1M KOH, 1 M Na_2SO_4 and 0.5 M H_2SO_4, (b) SEM image of V_2C/BVO and (c) EDS elemental mapping of V_2C/BVO after stability test, (d) XPS survey spectra of V_2C/BVO after HER stability, High-resolution XPS spectra of V_2C/BVO after HER stability: (e) V2p, (f) C1s, and (g) Bi4f, (h) The Nyquist plots of V_2C/BVO before and after stability.

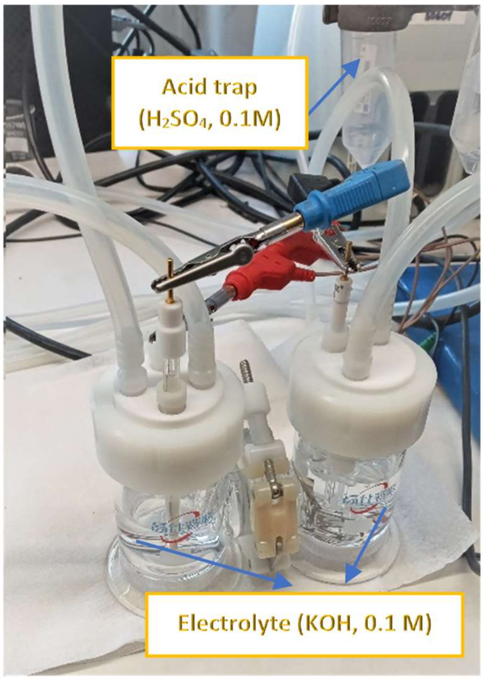

Fig. S8 Photograph of H-type electrochemical cell.

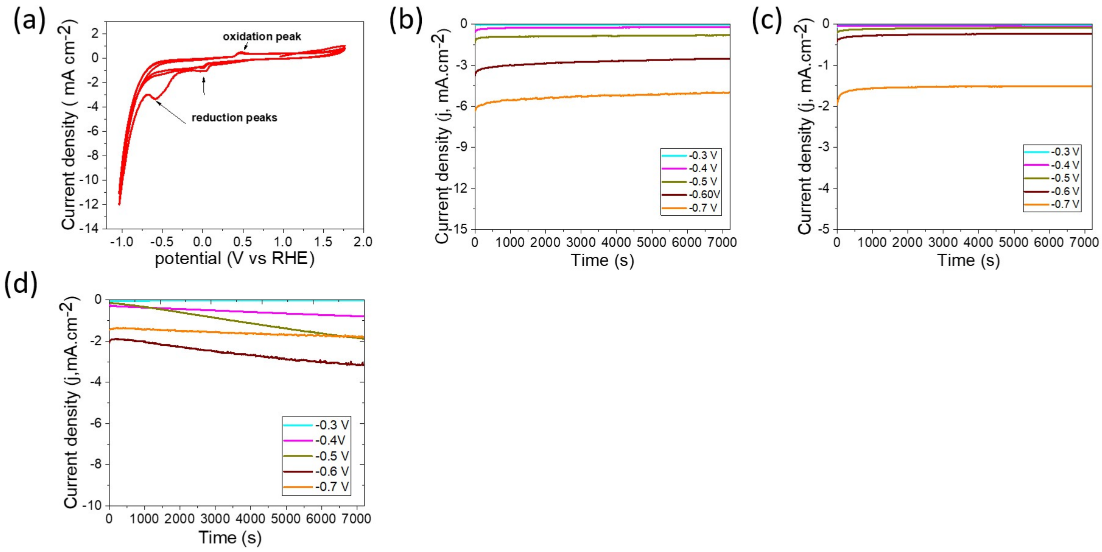

Fig S9 (a) Three consecutive CV scans of V_2C/Bi in 0.1 M KOH under N_2, Chronoamperometry curves of diverse applied potentials for (b) V_2C/Bi, (c) V_2C/BVO and (d) V_2C.

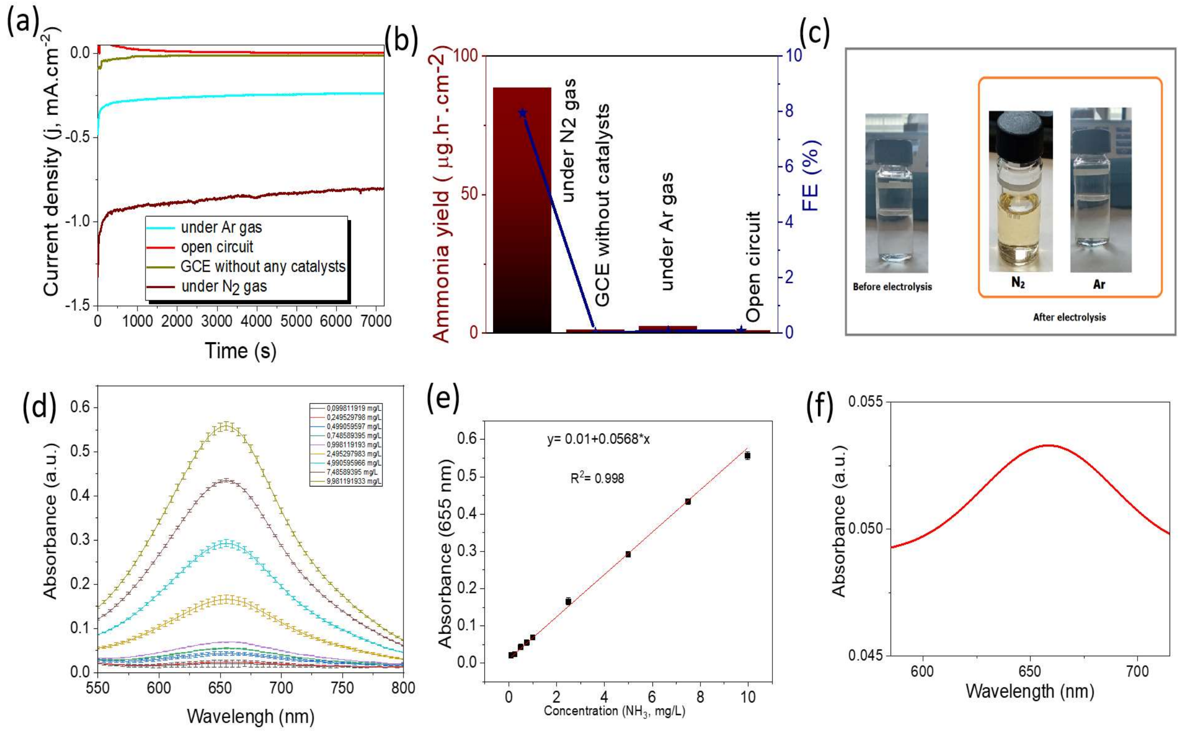

Fig. 10 (a) Chronoamperometry curves of V_2C/Bi under different electrochemical conditions, (b) Ammonia yield and corresponding FE after 2h NRR under different conditions (c) images of a solution derived from an electrolyte before and after NRR test using N_2 and Ar as feeding gas on the V_2C/Bi electrode detected using the NH_3 color reagent, (d) UV-Vis curves of indophenol assays after incubated for 2 hours, (e) calibration curve used for estimation of NH_3 concentration. The absorbance at 655 nm was measured by UV-Vis spectrophotometer, and the fitting curve shows good linear relation of absorbance with NH_3 concentration ($y = 0.0568x + 0.01$, R^2=0.998), and (f) UV-vis absorption spectra of NH_3 concentration.

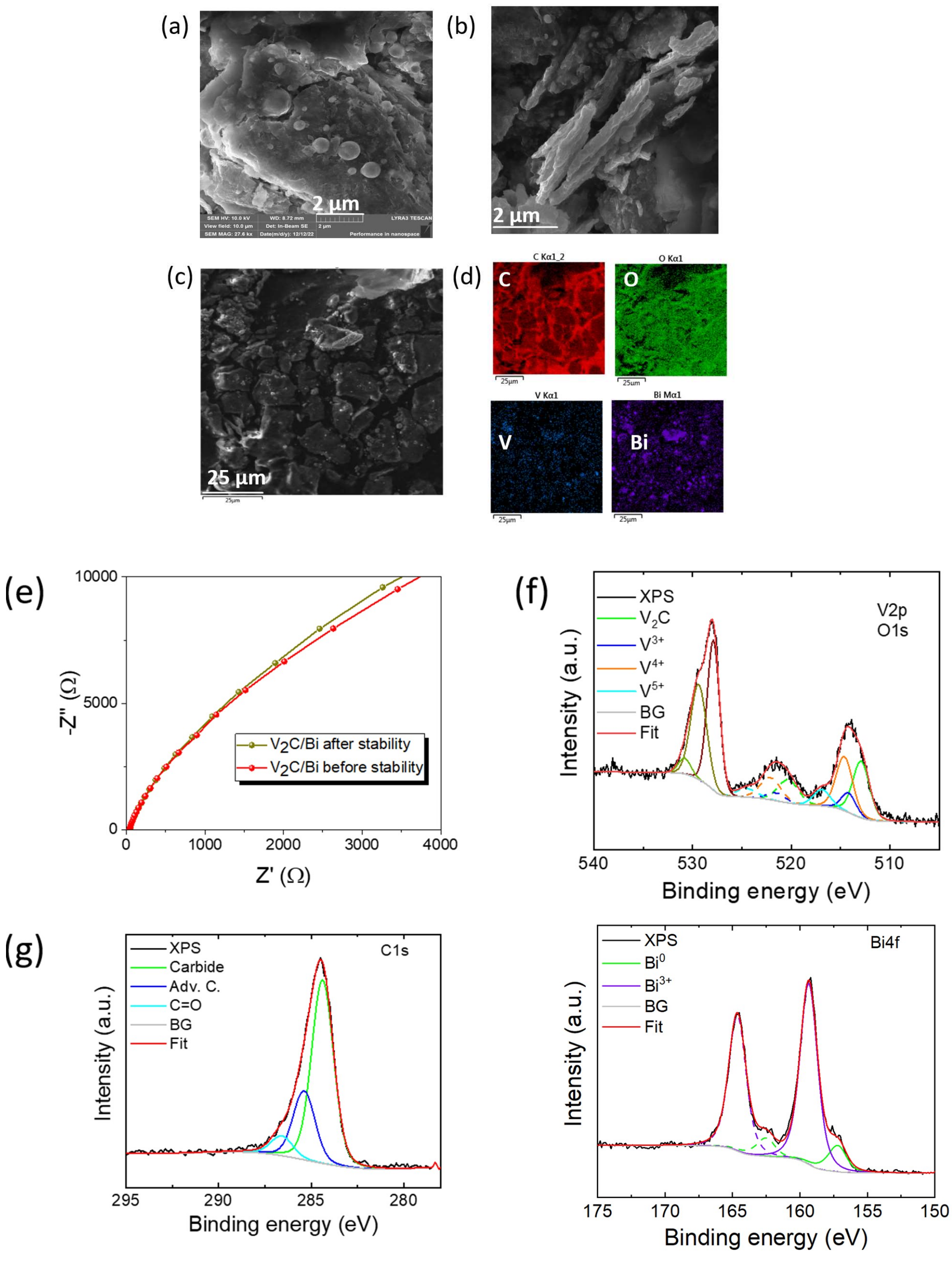

Fig. S11 (a, b, c) SEM images of V_2C/Bi after the 24 h stability test and (d) the corresponding EDS element mapping, (e) The Nyquist plots of V_2C/Bi before and after stability, High-resolution XPS spectra of V_2C/Bi after NRR stability: (f) V2p, (g) C 1s, and (h) Bi 4f.

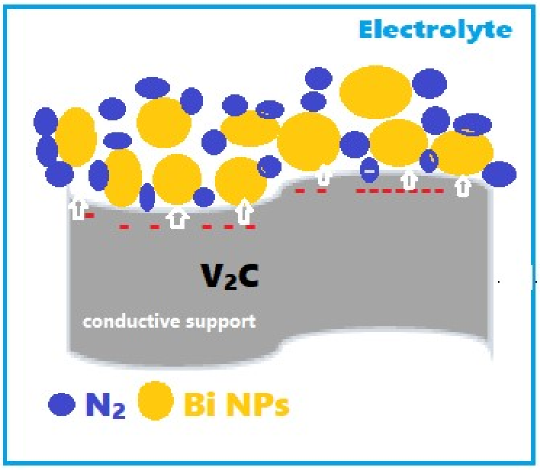

Fig. S12 Schematic of electron transfer between Bi and V_2C and adsorption sites of N_2.

Table S1 Elements detected from XPS measurement.

Elements	V	C	O	F	Bi
Atomic percent V_2C	17.36	37.5	26.3	18.5	-
Atomic percent V_2C/BVO	11.8	24.4	43.6	8	11.2
Atomic percent V_2C/Bi	11.54	26.8	43.77	11.3	6.8

Table S2 comparison of η_{10} values with other non-noble metal catalysts.

Catalysts	Overpotentials (mV)	References
V_2C/BVO	384	This work
Se/Ti_3C_2	712	2D Mater. 9 (2022) 045019
Te / Ti_3C_2 S/ Ti_3C_2	690 830	Nanoscale, 15 (2023) 4033–4044
Ni NPs@N-Nb_2CT_x	720	Small 19 (2023) 2206098
MoS_2/Ti_3C_2	400	Int. J. Hydrogen Energy 44 (2019) 965-976
$Nb_4C_3T_x$-180	398	Int. J. Hydrogen Energy 46 (2021) 1955-1966
CoMoP@C	448	Energy Environ. Sci. 10 (2017) 788
VS_2 nanoflowers	400	Int. J. Hydrogen Energy 43 (2018) 22949-22954
Ti_3C_2 flakes	385	ACS Sustainable Chem. Eng. 6 (2018) 8976−8982
$Bi_{1.85}Sr_2Co_{1.85}O_{7.7-\delta}$	589	ChemPhysChem 16 (2015) 769-774
V_2CT_x	618	Appl. Surf. Sci. 582 (2022) 152481
VSe_2	414	ACS Appl. Energy Mater. (2019) 644−653

Table S3 Comparison of the electrocatalytic NRR performance of V_2C/Bi with other NRR aqueous-based NRR electrocatalysts at ambient conditions.

Catalyst	Electrolyte	NH_3 yield	FE (%)	Ref.
V_2C/Bi	0.1 M KOH	88.6μg h^{-1} cm^{-2}	8	This work
Ni/Nb_2C	0.1 M KOH	26.16 μg h^{-1} cm^{-2}	7.3	Ceram. Int. 2022, 48, 20599
Cu/Ti_3C_2	0.1 M KOH	3.04 μmol h^{-1} cm^{-2}	7.31	ChemPlusChem 2021, 86, 166
$Ti_3C_2T_x$	0.01 M Na_2SO_4	2.81× 10^{-5} μmol·s -1 ·cm^{-2}	7.4	Nano Converg. 2021, 8, 14
NS-$Ti_3C_2T_x$	0.05 M H_2SO_4	34.23 μg h^{-1} mg^{-1}_{cat}	6.6	J. Alloys Comp. 2021, 869, 159335
V_2CT_x	0.1 M Na_2SO_4	12.6 μg h^{-1} cm^{-2}	4	Catal. Lett. 2021, 151, 3516
TiO_2/$Ti_3C_2T_x$	0.1M HCl	26.32 μg h^{-1} mg^{-1}_{cat}	8.42	Inorg. Chem. 2019, 58, 5414
V_2CT_x	0.1M HCl	25.1 μg h^{-1} mg^{-1}_{cat}	11.7	Catal. Lett. 2021, 151, 3516

$Ti_3C_2T_x$	0.1 M H_2SO_4	20.4 μg h^{-1} mg^{-1}_{cat}	9.3	J. Mater. Chem. A, 2018, 6, 24031
$MnO_2/Ti_3C_2T_x$	0.1 M HCl	34.12 μg h^{-1} cm^{-2}	11.39	Mater. Chem. A, 2019, 7, 18823
$Ti_3C_2T_x$ /FeOOH	0.5 M Li_2SO_4	0.26 μg h^{-1} cm^{-2}	5.78	Joule 2019, 3, 279
$Mn_3O_4/Ti_3C_2T_x$	0.1 M Na_2SO_4	25.95 μg h^{-1} cm^{-2}	5.51	Chem. Eng. J., 2020, 396
$RuFe@Ti_3C_2T_x$	0.1 M KOH	40.79 μg h^{-1} cm^{-2}	15.25	ChemCatChem 2022, 14, e202101775